A Robust Short-circuit Calculation Method for Islanded, Grid-connected, and Utility Microgrids

Luka V. Strezoski, *Senior Member*, *IEEE*, Nikola G. Simic, *Student Member*, *IEEE*, and Kenneth A. Loparo, *Life Fellow*, *IEEE*

***Abstract*——In this paper, a robust method for quantifying the impact of short-circuit faults on microgrids is proposed. Microgrids can operate in both islanded (grid-forming) and grid-connected (grid-following) modes, and the ownership and responsibility for the microgrid operation can vary significantly from distribution system operators (DSOs) to third-party microgrid operators. This necessitates the development of a robust short-circuit calculation (SCC) method that can provide accurate results for all the possible microgrid topologies, operational modes, and ownership models. Unlike previously developed SCC methods for microgrids, the SCC method proposed in this paper provides highly accurate results for all possible microgrid topologies: islanded microgrid, grid-connected microgrid, and utility microgrid as a part of a larger distribution grid. In addition, the proposed SCC method solves the short-circuit faults of any complexity, with the same simplicity. The proposed SCC method is tested on a complete model of a real-life microgrid on the Case Western Reserve University campus, operating in both islanded and grid-connected modes. The computational results show the advantages of the proposed SCC method in comparison to the previous ones for microgrids, regarding the robustness (ability to solve complex short-circuit faults with an arbitrary number of faulted buses and phases that affect a microgrid of any topology), as well as the accuracy of the results.**

***Index Terms*—Distributed energy resource, short-circuit fault, microgrid, short-circuit calculation.**

I. Introduction

THE objective of this paper is to develop a robust and accurate short-circuit calculation (SCC) method applied to microgrids, which may be affected by any types of complex short-circuit faults, regardless of their operational state, topology, and ownership. A complex short circuit, in the context of this paper, is defined as any type of single or simultaneous short circuit, solid short circuit, or short circuit through impedances, with an arbitrary number of faulted buses and phases [1]. The SCC plays a pivotal role in power system analysis and numerous other power applications, including: ① protection setting, coordination, and sensitivity analysis of relays; ② the arc-flash analysis; ③ the calculation of inrush currents and the selection of power system equipment; and ④ the fault location, isolation, and supply restoration (FLISR). Thus, it is essential to have a robust and accurate SCC method for every level of electric power systems, including transmission and distribution grids as well as rapidly emerging microgrids.

SCC methods are well-established for transmission grids and have been successfully applied in the last several decades [2]-[4]. As transmission grids are heavily meshed and the number of nodes is not as large as in distribution grids, the transmission grid modeling and calculations are bus-oriented and performed using the system nodal admittance matrix and its implicit inverse (using factorization) [2]-[4]. For distribution grids, which are characterized by the radial structure, large numbers of nodes, and frequent topology changes, a new class of SCC methods has been developed [5]-[9]. These methods are branch-oriented and do not require building and factorizing the system nodal admittance matrix. However, with significant improvements in computational capability over the last decade and the realization that the main issue with bus-oriented SCC methods lies in the required computational effort to build and factorize the impedance matrix, the applications of bus-oriented SCC methods to distribution grids are gaining attention in the last several years [10]-[12].

For microgrids, which are the focus of this paper, it is essential to consider several important and unique features of the topology and structure. First, microgrids can operate in distinct modes, and the fault currents inside the microgrid may differ significantly depending on the operational mode [13]-[18]. In the grid-connected mode, the highest fault current originates from the utility grid connected to the microgrid, while distributed energy resources (DERs) inside the microgrid contribute to no more than 20% of the total fault current [13]. Conversely, in the islanded mode, the entire fault current is supplied by DERs inside the microgrid, and consequently, the total fault current is several times lower than that in the grid-connected mode [13]-[16]. Further, microgrids can be owned, managed, and controlled by different stakeholders [19]. When a microgrid is part of the utility grid and a distribution system operator (DSO) is responsible for its operation, which is called utility microgrid, most of the calculations are performed on the entire grid model incor-

Manuscript received: December 31, 2023; revised: April 13, 2024; accepted: July 4, 2024. Date of CrossCheck: July 4, 2023. Date of online publication: August 26, 2024.

L. V. Strezoski (corresponding author) and N. G. Simic are with the Faculty of Technical Sciences, University of Novi Sad, Novi Sad, Serbia (e-mail: lukastrezoski@uns.ac.rs; nikola.simic@uns.ac.rs).

K. A. Loparo is with the EECS Department at Case Western Reserve University, Cleveland, USA (e-mail: kal4@case.edu).

DOI: 10.35833/MPCE.2023.001041

porating the microgrid as part of the larger distribution grid. In this case, an SCC method should be able to efficiently calculate the fault current flow in the entire distribution grid. When a microgrid is owned and operated by a third-party entity and operates in the grid-connected mode, only the microgrid is modeled, and the contribution of utility grid to the fault current is represented with its Thevenin equivalents [13] - [15]. Thus, in SCCs, only the contribution of utility grid to the fault current inside the microgrid is considered, whereas the rest of the utility grid is not modeled. When a microgrid operates in an islanded mode, regardless of its ownership, only the microgrid is modeled, and the utility grid has no impact on the operation of microgrid [16] - [18]. SCC method should be applicable to: ① a grid-connected microgrid; ② a utility microgrid that is part of a larger distribution grid; or ③ an islanded microgrid that operates independent of the utility gird, and must be capable of efficiently coping with all these cases and providing accurate results for any possible complex short-circuit fault that may occur inside the microgrid.

II. Literature Review and Problem Statement

This section presents a comprehensive overview of the current state-of-the-art in SCC methods across various parts of a power system. This analysis, coupled with identified gaps in existing literature, forms the basis for defining the motivation, objectives, and key contributions of this paper.

SCC methods for distribution grids are predominantly branch-oriented [5] - [9] and do not require building and factorizing the nodal admittance matrix of distribution grid, thereby making the real-life computation efficient. A hybrid compensation method (HCM) is used for SCC in [5] and [6]. This procedure uses a compensation technique for solving the short-circuit currents, loop currents, and currents injected by synchronous machines. A backward/forward sweep (BFS) calculation procedure is then applied to calculate the complete network state. For every short-circuit fault to be analyzed, the HCM needs to predefine the specific fault conditions by deriving particularly complex equations, which may hinder its implementation in industrial software tools because of the computational burden. BFS methods are designed for distribution grids but they require a stiff slack-bus (network root) to work properly, which may result in computational issues in the context of islanded microgrids, as discussed in [13]. Additionally, the HCM assumes that synchronous machines are the only active elements in the power system. This is not the case for microgrids, where most DERs, e.g., solar photovoltaics (PVs), wind turbines (WTs), and energy storage (ES), are electronically connected and cannot be modeled as traditional synchronous machines. Thus, fundamentally different modeling and integration approaches are required [20]-[22]. In [7] and [8], an SCC method in the phasor domain is proposed based on bus-current-injections to branch-current (BIBC) and branch-current to bus-voltage (BCBV) matrices. However, this method is burdened with the same shortcomings as the aforementioned ones. In [1] and [9], the improved backward/forward sweep (IBFS) method in the sequence domain is proposed for the SCC of distribution grids with all types of DERs. In [9], all types of DERs are integrated into the SCC through the novel concept of the generalized Δ-circuit. The method in [9] only deals with standard types of solid short-circuit faults, whereas the method in [1] can be applied to any type of complex short-circuit faults, without predefining boundary conditions for each of different fault types. However, like the HCM, the IBFS method in both [1] and [9] may have difficulty in performing SCCs for islanded microgrids without a specified network root [13]. As previously discussed, the impedance matrix based SCC methods for distribution grid are receiving increased attention as the available computational power increases [10]-[12]. However, the efficient impedance matrix based methods also require predefining specific fault conditions for each of different fault types, and thus they may not be sufficiently robust for industrial SCC tools.

The state-of-the-art SCC methods for microgrids are much less developed than those for transmission and distribution grids as previously described. In [14], a fault occurring in a grid-connected microgrid is analyzed, using the real-time digital simulator (RTDS). The RTDS performs its calculations in the time domain, and thus it is not suitable for online calculations, where the SCC results are required in a range of milliseconds and multiple SCCs need to be sequentially analyzed (e.g., for adaptive relay protection or FLISR) [23]. Also, it is limited to standard and solid short-circuit faults and is unable to compute complex short-circuit faults. In [15], an SCC method for grid-connected microgrids is analyzed using the power system analysis toolbox (PSAT). However, the SCC method used in the PSAT is designed for distribution grids, which is limited to solid short-circuit faults, and may not be applicable for islanded microgrids. In [16] and [17], the electro-magnetic transient program (EMTP) is utilized, having the same limitations as the one in [14] due to its reliance on a time-domain simulation. In [18], an SCC method for islanded microgrids is proposed, but it requires predefining fault conditions for each of different fault types and has not been tested for grid-connected microgrids. The SCC method proposed in [23] is designed specifically for droop-controlled and islanded microgrids and not aimed for grid-connected nor utility microgrids. To the best of our knowledge, this method is the only one that does not require the existence of a slack bus. However, it introduces a virtual slack bus, which has to be modeled and the voltage variation of which has to be considered. Moreover, similar to previous methods, [23] also requires predefining the fault conditions for each of different fault types.

To the best of our knowledge, the only two SCC methods developed to date that do not require predefining the fault conditions for each of different fault types are in [1] and [4]. However, the SCC method in [4] is developed for traditional transmission grids, where the only active elements are synchronous machines, and the traditional superposition theorem is used to decompose the faulted state into the pre-fault and traditional (passive) Δ-circuit states. As shown in [9], the passive Δ-circuit cannot be used for modeling grids that contain electronically-coupled DERs, such as emerging mi-

crogrids. The SCC method proposed in [1] does not have the aforementioned limitation as it is based on the generalized Δ-circuit concept that allows the integration of electronically-coupled DERs into the SCC, but as discussed above, the SCC method in [1] is based on the IBFS method and is of limited use for islanded microgrids without a specified network root.

The motivation for this paper is the lack of robust methods capable of performing SCCs in faulted microgrids, regardless of their operational mode, topology, and ownership, without the need to predefine boundary conditions for short-circuit faults of any complexity. The main objectives are as follows.

1) Improve the modeling of complex short-circuit faults from [1] to facilitate the application to microgrids affected by any type of complex short-circuit fault.

2) Develop an admittance matrix based SCC method that can be applied to microgrids in the grid-connected and islanded modes, as well as those integrated into larger distribution grids.

3) Integrate accurate models for DERs, including traditional and electronically-coupled DERs, into the proposed SCC method for microgrids.

Following these objectives, a robust and efficient SCC method for faulted microgrids is developed in this paper. The contributions of the proposed SCC method are as follows.

1) The proposed SCC method can be applied to faulted microgrids, regardless of their operational mode, ownership, or topology.

2) The proposed SCC method does not require a network root, and thus overcomes the issues of traditional SCC methods when a microgrid is operating in the islanded mode.

3) The proposed SCC method solves all types of complex short-circuit faults without requiring a complicated derivation of boundary conditions for each of different fault types, and thus it can be readily integrated into industrial software tools for performing SCCs.

4) The proposed SCC method is computationally efficient and suitable for online calculations in real-life systems and can also be implemented in advanced applications such as adaptive relay protection and FLISR.

The proposed SCC method is tested on a model of a real-life microgrid on the Case Western Reserve University (CWRU) campus, with different short-circuit faults simulated in various nodes. Both islanded and grid-connected modes are considered. To further study the applicability of the proposed SCC method, it is also tested on a utility microgrid as a part of a larger distribution grid. The computational results of these experiments are provided and clearly demonstrate the advantages of the proposed SCC method in comparison to previous ones.

The remainder of this paper is organized as follows. In Section III, different microgrid topologies are discussed and DER modeling for SCC purposes is presented. In Section IV, the complex short-circuit faults are discussed and their mathematical models are derived. In Section V, a microgrid affected by complex short-circuit faults is discussed and modeled. The proposed SCC method is presented in Section VI, while the numerical results are presented and discussed in Section VII. This paper is concluded in Section VIII.

III. Microgrid Topology and DER Modeling

According to the definition by the US Department of Energy, a microgrid is "A group of interconnected loads and DERs with clearly defined electrical boundaries that acts as a single controllable entity with respect to the grid and can connect and disconnect from the grid to enable it to operate in both grid-connected or islanded modes" [24].

A. Microgrid Topology

A microgrid should be able to operate as an autonomous system, i.e., in islanded mode without connection to the utility grid, as well as in the grid-connected mode, where the utility grid maintains the stability of the entire system. The characteristics of the fault current flows are very different in these two operational modes [13]. Furthermore, depending on the ownership and operational responsibility for the microgrid, the utility grid connected to the microgrid may need to be fully modeled or its Thevenin equivalent may be a sufficient model in a grid-connected mode. If a microgrid is owned and operated by a third party that is not a part of the utility grid to which the microgrid is connected, the impact of the utility grid on the fault current flow inside the microgrid is modeled with its Thevenin equivalent [13]-[15]. If a microgrid is owned and operated by a DSO, who is responsible for maintaining stability and reliability of the entire grid including the utility microgrid as a part of a larger distribution grid, the entire grid should be properly modeled and the fault current flow through the entire grid is of importance [25]. Thus, there are three distinct cases that need to be considered in developing a robust SCC method aimed for microgrids.

1) Case 1: islanded microgrid.

2) Case 2: grid-connected microgrid, owned and controlled by a third-party operator.

3) Case 3: utility microgrid, owned and operated by a DSO.

The three cases are depicted in Fig. 1, where the microgrid on the CWRU campus is shown, and DG is short for diesel genset. Additional details and parameter values are presented in Section VI [26]. The load from the original microgrid has been modified in this paper, in order to be serviceable by the available generation, as explained in Section VI. In Fig. 1(a), cases 1 and 2 are distinguished depending on the switch status of the main circuit breaker (MCB).

Finally, if it is a utility microgrid as part of a larger distribution grid (case 3), the matrix consists of the entire grid including the microgrid. The equation that connects the voltages and injected currents through the admittance matrix of the modeled (micro)grid is expressed as:

$$\hat{\boldsymbol{Y}}\hat{\boldsymbol{U}} = \hat{\boldsymbol{J}}_{INJ} \tag{1}$$

where $\hat{\boldsymbol{Y}}$ is the admittance matrix; $\hat{\boldsymbol{U}}$ is the vector of nodal voltages; and $\hat{\boldsymbol{J}}_{INJ}$ is the vector of injected currents.

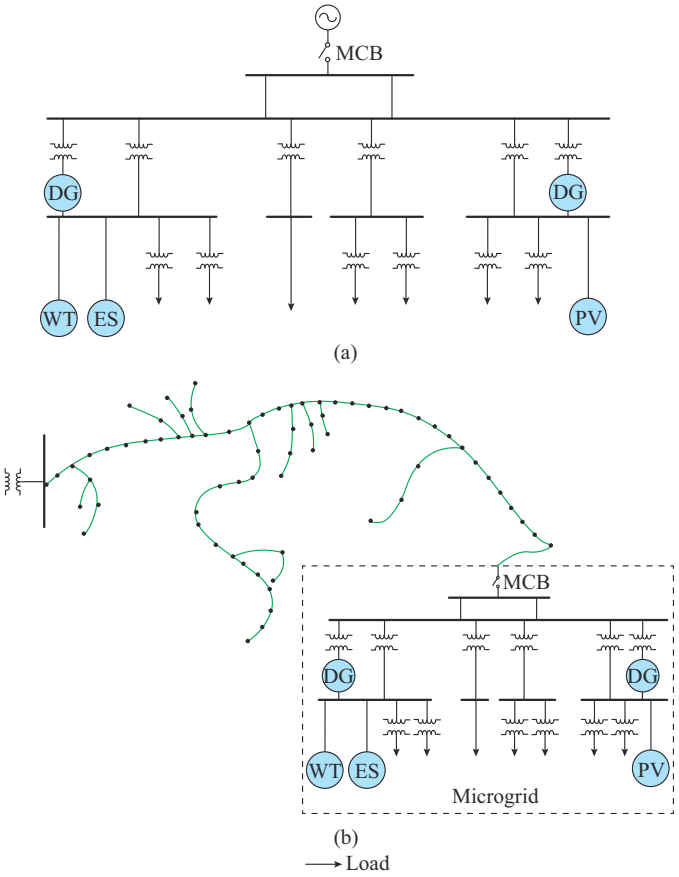

Fig. 1. Structure of cases 1-3. (a) Cases 1 and 2. (b) Case 3.

B. DER Modeling

For the SCC, DERs can be divided into those directly connect to the grid (traditional synchronous and induction machines) and those that are electronically-coupled inverter-based DERs (IBDERs) including PVs, WTs, ES, etc. [1], [9], [20]-[22]. Synchronous and induction machines directly connected to the grid are modeled with ideal voltage sources behind sub-transient, transient, or steady-state impedances. This model can accurately represent the fault response of traditional machines, which completely depends on the physical characteristics of the machines [1]-[8]. Integrating this model into traditional SCC methods is straightforward. The faulted state is decomposed into the pre-fault and the Δ-circuit states. The ideal voltage sources are nulled in the Δ-circuit and their impact is recognized from the pre-fault state, and the impedances of the machines are included in the admittance matrix of Δ-circuit model [1]-[8]. Thus, the Δ-circuit is passive everywhere except at the fault location, which facilitates the computations. When IBDERs are considered, they cannot be integrated into the SCC using a traditional (passive) Δ-circuit concept [9], [20]-[22]. This is because their short-circuit currents are not dictated by their physical characteristics, but rather by the control strategies implemented on the inverters through which IBDERs are connected to the grid. The fault currents of IBDERs are controlled and limited and their values are different from their pre-fault values, so it is not possible to accurately represent the faulted state by decomposing it into the pre-fault state and the Δ-circuit state. In [9], a generalized Δ-circuit concept is proposed that allows the inclusion of IBDERs by injecting so-called excess currents into the generalized Δ-circuit in every node where an IBDER is connected.

The excess current of IBDER $\hat{I}^{\Delta+}_{\mathrm{IBDER}l}$ is calculated as:

$$\hat{I}^{\Delta+}_{\mathrm{IBDER}l}=\hat{I}^{\mathrm{f}}_{\mathrm{IBDER}l}-\hat{I}^{\mathrm{pf}}_{\mathrm{IBDER}l} \quad l\in\alpha_{\mathrm{IBDER}} \tag{2}$$

where l and α_{IBDER} are the index and set of nodes where IBDERs are connected to the grid, respectively; $\hat{I}^{\mathrm{f}}_{\mathrm{IBDER}l}$ is the fault current of IBDER; and $\hat{I}^{\mathrm{pf}}_{\mathrm{IBDER}l}$ is the pre-fault current obtained from power flow or state estimation.

To calculate $\hat{I}^{\mathrm{f}}_{\mathrm{IBDER}l}$, the modeling procedure from [20] is used in this paper. Briefly, the modeling procedure consists of a pre-iteration step, in which the fault voltages at the nodes where IBDERs are connected to the grid are estimated. Based on these voltages as well as the low-voltage ride through (LVRT) and reactive current injection (RCI) requirements for the IBDERs, as determined by the control strategies implemented in the inverters of IBDERs, the required reactive component for the fault current of IBDER is calculated. Finally, based on the known fault current limit of the inverter, the active component for the fault current of IBDER is calculated. It should be noted that this modeling procedure does not depend on detailed information from the manufacturer. Thus, it can be used when the information from the manufacturer is unavailable or only partially available. If the control strategy of IBDER implies virtual impedance current limiters, the modeling will be slightly different. Briefly, the positive-sequence component is modeled by a virtual impedance and a voltage source, whereas the negative- and zero-sequence components are modeled with two virtual impedances. The first step is transforming positive-sequence Thevenin equivalent of IBDER into Norton equivalent, which has an ideal current source and a parallel impedance. The current from the ideal source is considered as the excess current at the node where the IBDER is connected, whereas positive-, negative-, and zero-sequence impedances are included in the admittance matrix of Δ-circuit model.

IV. Complex Short-circuit Faults

Any type of a complex short-circuit fault can be accurately modeled with one or several fault modules associated with the pre-fault model of microgrid [1], [9].

A. Fault Module

As illustrated in Fig. 2(a), a fault module is comprised of the following components.

1) Five nodes: phase nodes a, b, and c, neutral node n, and a ground node G. Nodes a, b, and c are the connection points between the fault module and the microgrid.

2) Four branches with impedances $\hat{Z}_{ja}$, $\hat{Z}_{jb}$, $\hat{Z}_{jc}$, and $\hat{Z}_{jn}$, where j is the index of fault module, and six ideal voltage sources with the pre-fault phase voltages of bus k $\hat{U}^{\mathrm{pf}}_{ka}$, $\hat{U}^{\mathrm{pf}}_{kb}$, and $\hat{U}^{\mathrm{pf}}_{kc}$. On each branch, the two ideal voltage sources have the same magnitudes but opposite polarity.

The state of a fault module M_j is represented through a set of seven elements:

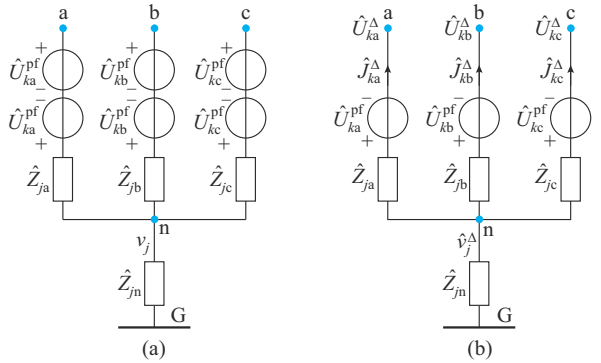

Fig. 2. Fault module and its Δ-circuit. (a) Fault module. (b) Δ-circuit.

$$M_j=\left\{\hat{Z}_{ja},\hat{Z}_{jb},\hat{Z}_{jc},\hat{Z}_{jn},\left(\hat{U}_{ka}^{pf}-\hat{U}_{ka}^{pf}\right),\left(\hat{U}_{kb}^{pf}-\hat{U}_{kb}^{pf}\right),\left(\hat{U}_{kc}^{pf}-\hat{U}_{kc}^{pf}\right)\right\} \tag{3}$$

The arbitrarily-selected complex short-circuit faults can be described by a set of N_1 appropriately selected fault modules as:

$$M=\left\{M_j,\ j=1,2,\ldots,N_1\right\} \tag{4}$$

B. Incidence Matrix

To model the connection between the fault modules and a microgrid, a $3N\times3N_1$ incidence matrix $\boldsymbol{T}$ is introduced. The matrix $\boldsymbol{T}$ is of block type, with the 3×3 block $\boldsymbol{T}_{kj}$ defined as:

$$\boldsymbol{T}_{kj}=\begin{cases}\boldsymbol{I} & \text{fault module } j \text{ is associated with faulted bus } k\\ \boldsymbol{0} & \text{fault module } j \text{ is not associated with faulted bus } k\end{cases} \tag{5}$$

where $j=1,2,\ldots,N_1$; $k=1,2,\ldots,N$, N is the number of buses in the modeled microgrid; and $\boldsymbol{I}$ and $\boldsymbol{0}$ are the 3×3 identity and zero matrices, respectively.

V. Faulted Microgrid

The model of faulted microgrid consists of all its elements (including traditional machines as well as IBDERs), with the associated fault modules described in Section III. In this paper, the faulted microgrid is analyzed by decomposing its state to the pre-fault state and generalized Δ-circuit state [9]. Because the pre-fault state is known, calculating the faulted state is reduced to calculating the generalized Δ-circuit state.

In the pre-fault state, all ideal voltage sources of the traditional machines and the voltage sources of the fault modules with positive polarity oriented toward the faulted buses are retained. They are nulled in the generalized Δ-circuit. The ideal current sources of IBDERs with their pre-fault currents are also retained.

In the generalized Δ-circuit, the active elements are the ideal voltage sources of the fault modules oriented from the faulted buses to the ground, as shown in Fig. 2(b), and the ideal current sources of IBDERs with the values of their excess currents. The fault module of the generalized Δ-circuit M_j^{Δ} is represented as:

$$M_j^{\Delta}=\left\{\hat{Z}_{ja},\hat{Z}_{jb},\hat{Z}_{jc},\hat{Z}_{jn},-\hat{U}_{ka}^{pf},-\hat{U}_{kb}^{pf},-\hat{U}_{kc}^{pf}\right\} \tag{6}$$

A. Mathematical Model of Generalized Δ-circuit of Fault Module

If the fault module j is associated with bus k (Fig. 2(b)), the state of its generalized Δ-circuit consists of two vectors and one scalar, i.e., $\hat{\boldsymbol{U}}_k^{\Delta}=[\hat{U}_{ka}^{\Delta},\hat{U}_{kb}^{\Delta},\hat{U}_{kc}^{\Delta}]^{\mathrm{T}}$, $\hat{\boldsymbol{J}}_j^{\Delta}=[\hat{J}_{ja}^{\Delta},\hat{J}_{jb}^{\Delta},\hat{J}_{jc}^{\Delta}]^{\mathrm{T}}$, and $\hat{v}_j^{\Delta}$.

The mathematical model of the generalized Δ-circuit for the fault module j associated with bus k in the phase domain can be derived as [1], [4]:

$$\begin{cases}\hat{\boldsymbol{A}}_j^{U}\hat{\boldsymbol{U}}_k^{\Delta}+\hat{\boldsymbol{A}}_j^{J}\hat{\boldsymbol{J}}_j^{\Delta}+\hat{\boldsymbol{A}}_j^{v}\hat{v}_j^{\Delta}=\hat{\boldsymbol{A}}_j^{0}\\ \hat{\boldsymbol{C}}_j^{J}\hat{\boldsymbol{J}}_j^{\Delta}+\hat{C}_j^{v}\hat{v}_j^{\Delta}=0\end{cases}\quad j=1,2,\ldots,N_1 \tag{7}$$

The parameters in (7) are defined as:

$$\left[\hat{\boldsymbol{A}}_j^{U}\right]_{3\times3}=\mathrm{diag}\left[\hat{A}_{ja}^{U}\ \ \hat{A}_{jb}^{U}\ \ \hat{A}_{jc}^{U}\right]\quad \hat{A}_{ji}^{U}=\begin{cases}0 & \hat{Z}_{ji}\to\infty\\ 1 & \text{otherwise}\end{cases} \tag{8}$$

$$\left[\hat{\boldsymbol{A}}_j^{J}\right]_{3\times3}=\mathrm{diag}\left[\hat{A}_{ja}^{J}\ \ \hat{A}_{jb}^{J}\ \ \hat{A}_{jc}^{J}\right]\quad \hat{A}_{ji}^{J}=\begin{cases}1 & \hat{Z}_{ji}\to\infty\\ \hat{Z}_{ji} & \text{otherwise}\end{cases} \tag{9}$$

$$\left[\hat{\boldsymbol{A}}_j^{v}\right]_{3\times1}=\left[\hat{A}_{ja}^{v}\ \ \hat{A}_{jb}^{v}\ \ \hat{A}_{jc}^{v}\right]^{\mathrm{T}}\quad \hat{A}_{ji}^{v}=\begin{cases}0 & \hat{Z}_{ji}\to\infty\\ -1 & \text{otherwise}\end{cases} \tag{10}$$

$$\left[\hat{\boldsymbol{A}}_j^{0}\right]_{3\times1}=\left[\hat{A}_{ja}^{0}\ \ \hat{A}_{jb}^{0}\ \ \hat{A}_{jc}^{0}\right]^{\mathrm{T}}\quad \hat{A}_{ji}^{0}=\begin{cases}0 & \hat{Z}_{ji}\to\infty\\ -\hat{U}_{ki}^{0} & \text{otherwise}\end{cases} \tag{11}$$

$$\left[\hat{\boldsymbol{C}}_j^{J}\right]_{1\times3}=\left[\hat{C}_{ja}^{J}\ \ \hat{C}_{jb}^{J}\ \ \hat{C}_{jc}^{J}\right]\quad \hat{C}_{ji}^{J}=\begin{cases}1 & \hat{Z}_{jn}\to\infty\\ \hat{Z}_{jn} & \text{otherwise}\end{cases} \tag{12}$$

$$\hat{C}_j^{v}=\begin{cases}0 & \hat{Z}_{jn}\to\infty\\ 1 & \text{otherwise}\end{cases} \tag{13}$$

where the subscript i corresponds to the three phases a, b, and c.

The mathematical model for the generalized Δ-circuit of the fault module in the sequence domain can be easily derived based on the model in (7), by multiplying the corresponding vectors and matrices with the transformation matrices $\hat{\boldsymbol{S}}$ and $\hat{\boldsymbol{S}}^{-1}$:

$$\begin{cases}\left(\hat{\boldsymbol{A}}_j^{U}\hat{\boldsymbol{S}}^{-1}\right)\left(\hat{\boldsymbol{S}}\hat{\boldsymbol{U}}_k^{\Delta}\right)+\left(\hat{\boldsymbol{A}}_j^{J}\hat{\boldsymbol{S}}^{-1}\right)\left(\hat{\boldsymbol{S}}\hat{\boldsymbol{J}}_j^{\Delta}\right)+\hat{\boldsymbol{A}}_j^{v}\hat{v}_j^{\Delta}=\hat{\boldsymbol{A}}_j^{0}\\ \left(\hat{\boldsymbol{C}}_j^{J}\hat{\boldsymbol{S}}^{-1}\right)\left(\hat{\boldsymbol{S}}\hat{\boldsymbol{J}}_j^{\Delta}\right)+\hat{C}_j^{v}\hat{v}_j^{\Delta}=0\end{cases}\quad j=1,2,\ldots,N_1 \tag{14}$$

The transformation matrix $\hat{\boldsymbol{S}}$ is defined as:

$$\hat{\boldsymbol{S}}=\frac{1}{3}\begin{bmatrix}1 & \hat{a} & \hat{a}^2\\ 1 & \hat{a}^2 & \hat{a}\\ 1 & 1 & 1\end{bmatrix}\quad \hat{a}=\mathrm{e}^{-\mathrm{j}\frac{2\pi}{3}} \tag{15}$$

Now, (14) can be written as:

$$\begin{cases}\underline{\hat{\boldsymbol{A}}}_j^{U}\underline{\hat{\boldsymbol{U}}}_k^{\Delta}+\underline{\hat{\boldsymbol{A}}}_j^{J}\underline{\hat{\boldsymbol{J}}}_j^{\Delta}+\hat{\boldsymbol{A}}_j^{v}\hat{v}_j^{\Delta}=\hat{\boldsymbol{A}}_j^{0}\\ \underline{\hat{\boldsymbol{C}}}_j^{J}\underline{\hat{\boldsymbol{J}}}_j^{\Delta}+\hat{C}_j^{v}\hat{v}_j^{\Delta}=0\end{cases}\quad j=1,2,\ldots,N_1 \tag{16}$$

where the symbol "_" corresponds to the element in the sequence domain.

B. Mathematical Model of Generalized Δ-circuit

The generalized Δ-circuit of the faulted microgrid can be modeled as:

$$\underline{\hat{\boldsymbol{J}}}_{INJ}^{\Delta}=\underline{\hat{\boldsymbol{Y}}}\,\underline{\hat{\boldsymbol{U}}}_{K}^{\Delta}+\boldsymbol{T}\,\underline{\hat{\boldsymbol{J}}}_{F}^{\Delta} \tag{17}$$

where $\underline{\hat{\boldsymbol{Y}}}$ is the admittance matrix of microgrid in the sequence domain; $\underline{\hat{\boldsymbol{J}}}_{INJ}^{\Delta}$ and $\underline{\hat{\boldsymbol{U}}}_{K}^{\Delta}$ are the $3N\times1$ vectors corresponding to the injected sequence currents and sequence voltages of all buses in the generalized Δ-circuit, respectively; $\underline{\hat{\boldsymbol{J}}}_{F}^{\Delta}$ is the $3N_1\times1$ vector corresponding to currents of all fault modules; and $\boldsymbol{T}$ is the $3N\times3N_1$ incidence matrix.

VI. Proposed SCC Method

As explained in Section II-B, due to the presence of IBDERs in the microgrid and the dependence of their fault currents on estimated voltages at their connection points at the moment of the fault occurrence, the proposed SCC method consists of two steps: ① pre-iteration step, in which the fault voltages at the connection points of all IBDERs are estimated; and ② calculation of the faulted state of microgrid. For both steps, the same SCC procedure is used, but with IBDERs modeled differently in each step, as explained in the following.

By combining (16) and (17), the mathematical model of the generalized Δ-circuit of the faulted microgrid is represented as (18) or in a more compact form as (19).

$$\begin{array}{c} \\ 3N \\ 3N_1 \\ N_1 \end{array}\!\!\begin{array}{c} \begin{array}{ccc} 3N & 3N_1 & N_1 \end{array} \\ \begin{vmatrix} \underline{\hat{\boldsymbol{Y}}} & \boldsymbol{T} & \boldsymbol{0} \\ \underline{\hat{\boldsymbol{A}}}^{U} & \underline{\hat{\boldsymbol{A}}}^{J} & \underline{\hat{\boldsymbol{A}}}^{v} \\ \boldsymbol{0} & \underline{\hat{\boldsymbol{C}}}^{J} & \hat{\boldsymbol{C}}^{v} \end{vmatrix} \end{array}\cdot\begin{array}{c} \begin{array}{c} 1 \end{array} \\ \begin{vmatrix} \underline{\hat{\boldsymbol{U}}}_{K}^{\Delta} \\ \underline{\hat{\boldsymbol{J}}}_{F}^{\Delta} \\ \hat{\boldsymbol{V}}^{\Delta} \end{vmatrix} \end{array}=\begin{array}{c} \begin{array}{c} 1 \end{array} \\ \begin{vmatrix} \underline{\hat{\boldsymbol{J}}}_{INJ} \\ \hat{\boldsymbol{A}}^{0} \\ \boldsymbol{0} \end{vmatrix} \end{array} \tag{18}$$

$$\hat{\boldsymbol{F}}\,\underline{\hat{\boldsymbol{X}}}^{\Delta}=\hat{\boldsymbol{F}}^{0} \tag{19}$$

The block of matrix $\underline{\hat{\boldsymbol{A}}}^{U}$ is defined as:

$$\underline{\hat{\boldsymbol{A}}}_{jk}^{U}=\begin{cases}\underline{\hat{\boldsymbol{A}}}_{j}^{U} & \text{fault module } j \text{ is associated with faulted bus } k\\ 0 & \text{fault module } j \text{ is not associated with faulted bus } k\end{cases} \tag{20}$$

The diagonal matrix $\underline{\hat{\boldsymbol{A}}}^{J}$ is defined as:

$$\underline{\hat{\boldsymbol{A}}}^{J}=\text{diag}\left[\underline{\hat{\boldsymbol{A}}}_{k}^{J}\right]\quad k\in\alpha_{\text{fault}} \tag{21}$$

where α_{fault} is the set of indices of faulted buses.

The matrices $\hat{\boldsymbol{A}}^{v}$ and $\underline{\hat{\boldsymbol{C}}}^{J}$ are defined as:

$$\begin{cases}\hat{\boldsymbol{A}}^{v}=\left[\hat{\boldsymbol{A}}_{1}^{v}\quad\hat{\boldsymbol{A}}_{2}^{v}\quad\cdots\quad\hat{\boldsymbol{A}}_{N_1}^{v}\right]\\ \underline{\hat{\boldsymbol{C}}}^{J}=\left[\underline{\hat{\boldsymbol{C}}}_{1}^{J}\quad\underline{\hat{\boldsymbol{C}}}_{2}^{J}\quad\cdots\quad\underline{\hat{\boldsymbol{C}}}_{N_1}^{J}\right]\end{cases} \tag{22}$$

The diagonal matrix $\hat{\boldsymbol{C}}^{v}$ is defined as:

$$\hat{\boldsymbol{C}}^{v}=\text{diag}\left[\hat{C}_{1}^{v}\quad\hat{C}_{2}^{v}\quad\cdots\quad\hat{C}_{N_1}^{v}\right] \tag{23}$$

The vector $\hat{\boldsymbol{V}}^{\Delta}$ is defined as:

$$\hat{\boldsymbol{V}}^{\Delta}=\left[\hat{v}_{1}^{\Delta}\quad\hat{v}_{2}^{\Delta}\quad\cdots\quad\hat{v}_{N_1}^{\Delta}\right]^{\mathrm{T}} \tag{24}$$

The vector $\hat{\boldsymbol{A}}^{0}$ is defined as:

$$\hat{\boldsymbol{A}}^{0}=\left[\left(\hat{\boldsymbol{A}}_{1}^{0}\right)^{\mathrm{T}}\quad\left(\hat{\boldsymbol{A}}_{2}^{0}\right)^{\mathrm{T}}\quad\cdots\quad\left(\hat{\boldsymbol{A}}_{N_1}^{0}\right)^{\mathrm{T}}\right]^{\mathrm{T}} \tag{25}$$

A. The First Step of SCC Procedure

In the first step, the aim is to estimate the voltages at the connection points of IBDERs at the moment of the fault occurrence, and it is assumed that all IBDERs inject their pre-fault currents. After the decomposition of the faulted state of microgrid to a pre-fault state and a generalized Δ-circuit state, the values of all IBDER currents in the generalized Δ-circuit state are null. Thus, the vector $\underline{\hat{\boldsymbol{J}}}_{INJ}$ in (18) is the zero vector, and the entire vector $\hat{\boldsymbol{F}}^{0}$ is known.

The vector of unknown variables $\underline{\hat{\boldsymbol{X}}}^{\Delta}$ in (19), which includes the short-circuit currents at the fault locations and the voltages of the faulted buses in the generalized Δ-circuit, is calculated as:

$$\underline{\hat{\boldsymbol{X}}}^{\Delta}=\hat{\boldsymbol{F}}^{-1}\hat{\boldsymbol{F}}^{0} \tag{26}$$

Note that in (26), the factorization of the matrix $\hat{\boldsymbol{F}}$ is used.

Once the vector $\underline{\hat{\boldsymbol{X}}}^{\Delta}$ is known, all the voltages in the faulted microgrid including the voltages at the connection points of IBDERs are calculated by superposition of the voltages in the generalized Δ-circuit state and the known pre-fault state. Finally, with the voltages at the connection points of IBDERs known, the excess currents of IBDERs are calculated following the procedure in [20].

B. The Second Step of SCC Procedure

When the excess currents of all IBDERs are known, the vector $\underline{\hat{\boldsymbol{J}}}_{INJ}$ is populated with their respective values at the connection points of IBDERs. The remaining elements in the vector $\underline{\hat{\boldsymbol{J}}}_{INJ}$ are null. In this step, the vector $\underline{\hat{\boldsymbol{J}}}_{INJ}$ is not a zero vector, but its values are known, and therefore vector $\hat{\boldsymbol{F}}^{0}$ is known as well.

The vector of unknown variables $\underline{\hat{\boldsymbol{X}}}^{\Delta}$ is calculated in (26) and contains values of all the voltages in the generalized Δ-circuit. The faulted state of microgrid is then calculated by superposition of the calculated generalized Δ-circuit state and the known pre-fault state. This concludes the SCC procedure and all the necessary variables for the faulted microgrid that have been calculated. The proposed SCC method is able to accurately calculate the state within both balanced (three-phase) and unbalanced (multi-phase) microgrids with complex faults. The flowchart of the proposed SCC method is presented in Fig. 3.

VII. Numerical Results

The proposed SCC method is initially tested on a fully modeled microgrid on the CWRU campus, as shown in Fig. 4 [26]. The microgrid consists of 28 three-phase buses, where bus 0 represents the point of common coupling (PCC) of microgrid to the utility grid. There are three different voltage levels within the microgrid: 11.2 kV, 0.48 kV, and 0.207 kV. The short-circuit power of utility grid is 1000 MVA with an *X/R* ratio of 22. The microgrid contains two DGs, each with rated power of 200 kVA, connected to buses 3 and 8, respectively. There are 3 IBDERs connected to buses 13, 14, and 21, respectively. Their nature and technology are explained in Fig. 4.

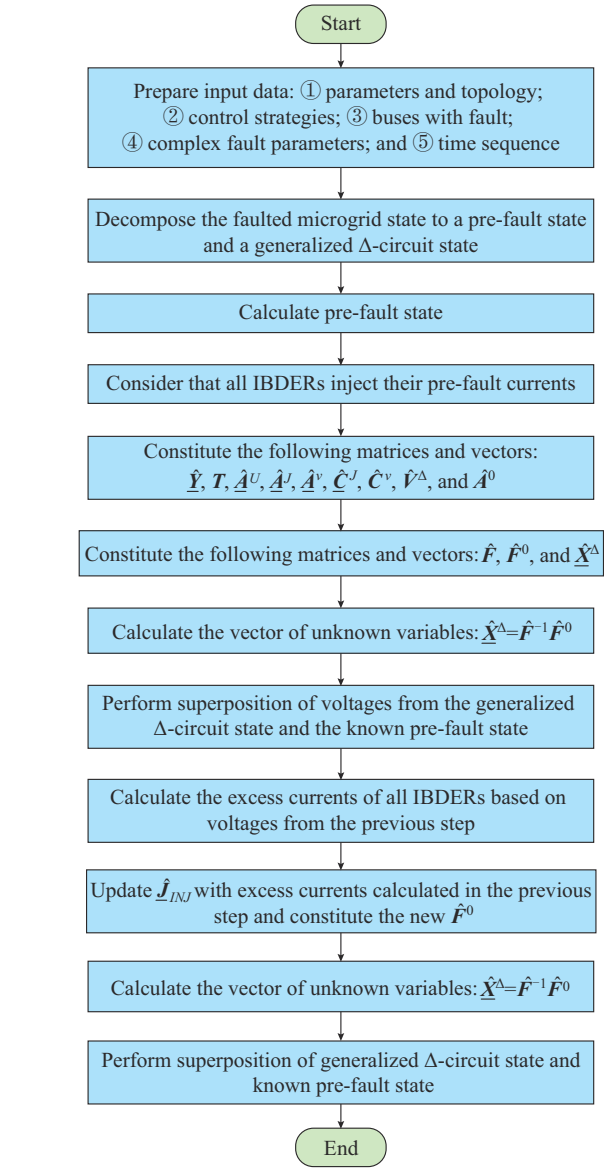

Fig. 3. Flowchart of proposed SCC method.

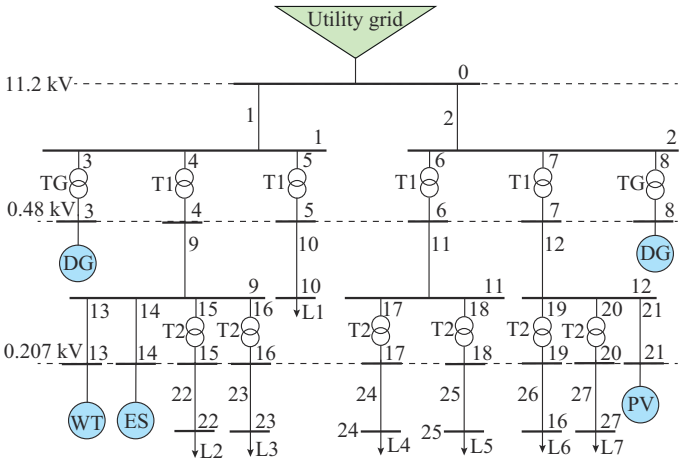

Fig. 4. Topology of microgrid on CWRU.

The rated power of WT is 60 kVA, and the rated power of ES and PV is 40 kVA. The impedances of lines 1, 2, 9, 10, 11, and 12 are the same and equal to (0.1608 + j0.0886)Ω/km. Lines 1, 2, 9, and 10 are 45.72 m, and lines 11 and 12 are 60.96 m. Lines 13, 14, 21, 22, 23, 24, 25, 26, and 27 have the same impedances equal to (0.1968 + j0.0984)Ω/km and all of them are 121.92 m.

The parameters for transformers TG, T1, and T2 are given in Table I. Further, a load of 40 kW (L1) is connected to bus 10 and several loads of 60 kW (L2-L7) are connected to buses 22-27, respectively. All elements are three-phase balanced.

TABLE I
PARAMETERS FOR TRANSFORMERS TG, T1, AND T2

Transformer	Connection type	Transformer ratio	Impedance voltage U_z (%)	Rated capacity	*X/R*
TG	Y/Y	11.2 kV/ 0.48 kV	5.75	2.0	6
T1	Y/Y	11.2 kV/ 0.48 kV	5.75	0.5	6
T2	Y/Y	0.48 kV/ 0.207 kV	5.75	0.5	3

To validate the accuracy of the proposed SCC method, the microgrid on CWRU campus is modeled using in-house developed software solution, coded in FORTRAN 2015, as well as a state-of-the-art hardware-in-the-loop (HIL) setup with connected (physical) inverter controller, implemented at the Smart Grid Laboratory, at the Faculty of Technical Sciences, University of Novi Sad [27]. The inverter controller connected to the HIL device has implemented the same LVRT and RCI control strategies as modeled in the IBDER in the FORTRAN code, and it is connected to bus 21 of the testbed microgrid. The inverter controller and the HIL device are depicted in Fig. 5.

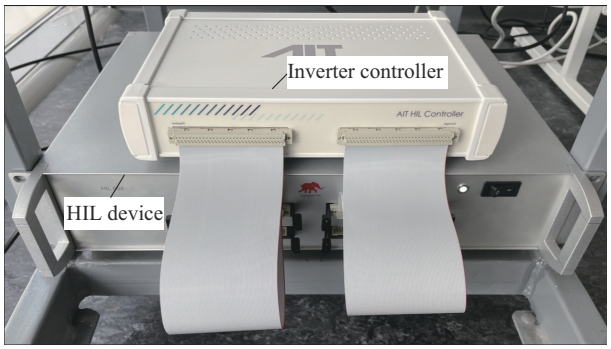

Fig. 5. Inverter controller and HIL device.

Five standard solid short-circuit faults, i.e., single-line-to-ground (SLG), two-line-to-ground (2LG), two-line (2L), three-line-to-ground (3LG), and three-line (3L) faults, are simulated at bus 11. Table II shows the currents on lines 1-27 I_1-I_{27} under 3LG fault with the proposed SCC method when the microgrid is in the grid-connected mode. To further validate the accuracy of the proposed SCC method, the same fault is implemented in the HIL setup, and the results are presented in Figs. 6 and 7. Due to the space limitations, only the results for a 3LG fault are presented here.

TABLE II
CURRENTS ON LINES 1-27 UNDER 3LG FAULT WITH PROPOSED SCC METHOD WHEN MICROGRID IS IN GRID-CONNECTED MODE

Fault current	Phase a		Phase b		Phase c	
	Magnitude (A)	Angle (°)	Magnitude (A)	Angle (°)	Magnitude (A)	Angle (°)
I_1	10.23	179.54	10.23	59.54	10.23	–60.46
I_2	338.29	–67.07	338.29	172.93	338.29	52.93
I_3	10.46	178.54	10.46	58.53	10.46	–61.46
I_4	1.86	–175.31	1.86	64.69	1.86	–55.31
I_5	2.05	–0.43	2.05	–120.43	2.05	–121.52
I_6	341.35	–65.90	341.35	174.10	341.35	54.10
I_7	2.81	–4.55	2.81	–124.55	2.81	115.46
I_8	10.45	178.43	10.45	58.42	10.45	–61.57
I_9	43.36	–175.31	43.36	64.69	43.36	–55.31
I_{10}	47.72	–0.43	47.72	–120.43	47.72	119.57
I_{11}	7964.93	–65.90	7964.93	174.10	7964.93	54.10
I_{12}	65.52	–4.55	65.52	–124.55	65.52	–115.45
I_{13}	108.98	179.92	108.98	59.92	108.98	–60.08
I_{14}	72.45	–179.91	72.45	60.08	72.45	–59.91
I_{15}	69.14	–1.49	69.14	–121.49	69.14	118.51
I_{16}	69.14	–1.49	69.14	–121.49	69.14	118.51
I_{17}	0	0	0	0	0	0
I_{18}	0	0	0	0	0	0
I_{19}	68.74	–2.20	68.74	–122.20	68.74	117.80
I_{20}	68.74	–2.20	68.74	–122.20	68.74	117.80
I_{21}	72.07	179.94	72.07	59.94	72.07	–60.06
I_{22}	160.32	–1.49	160.32	–121.49	160.32	118.51
I_{23}	160.32	–1.49	160.32	–121.49	160.32	118.51
I_{24}	0	0	0	0	0	0
I_{25}	0	0	0	0	0	0
I_{26}	159.41	–2.20	159.41	–122.20	159.41	117.80
I_{27}	159.41	–2.20	159.41	–122.20	159.41	117.80

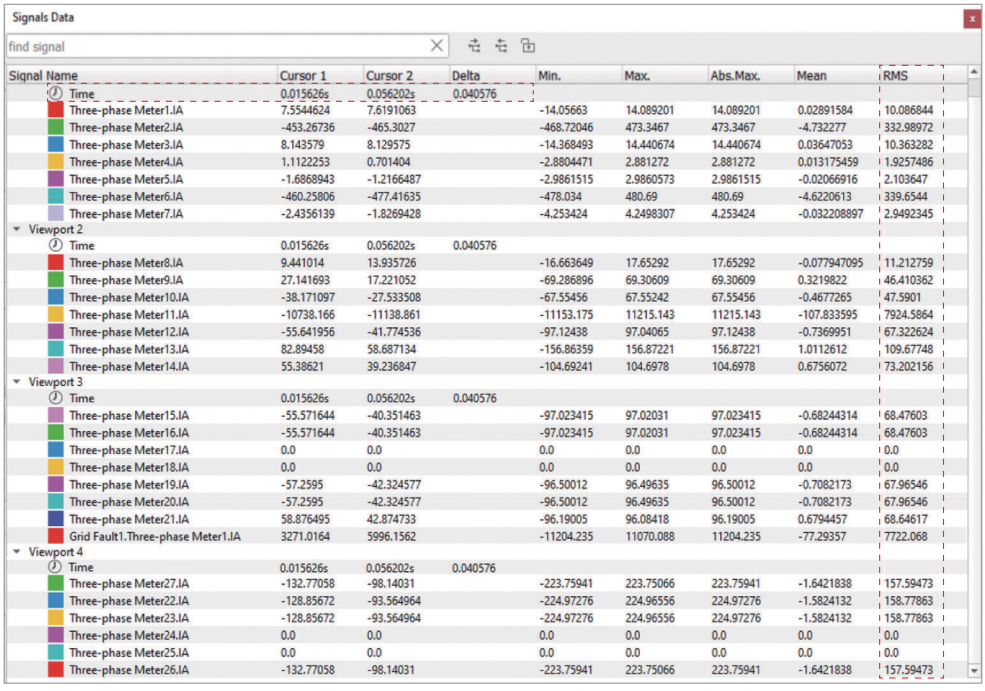

Fig. 6. Root mean square (RMS) values of currents on lines 1-27 under 3LG fault in HIL setup when microgrid is in grid-connected mode.

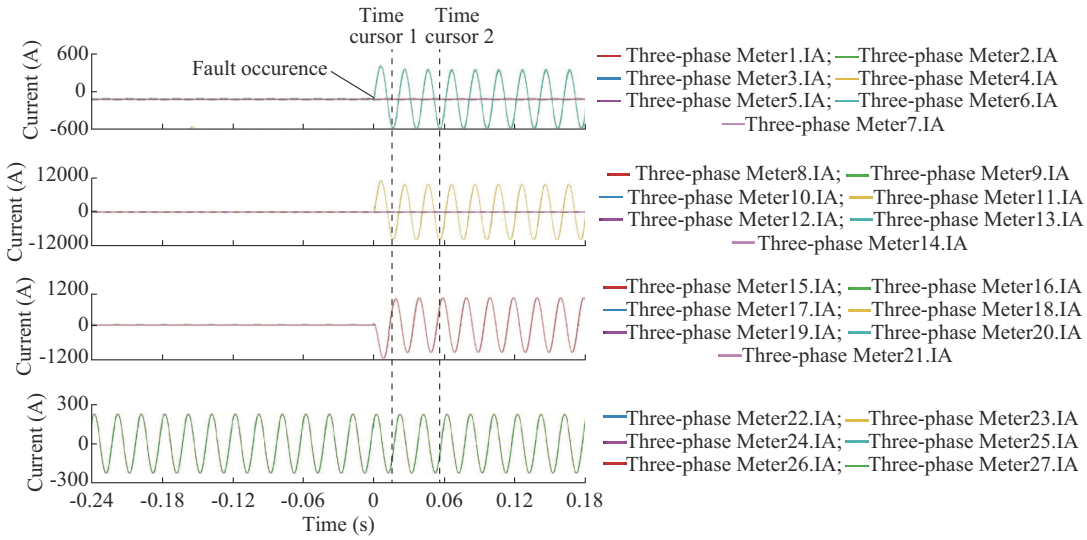

Fig. 7. Time-domain currents on lines 1-27 under 3LG fault in HIL setup when microgrid is in grid-connected mode

The RMS values in Fig. 6 are derived by analyzing signals from Fig. 7 in time period between time cursor 1 and time cursor 2. In the right-hand side of each sublot in Fig. 7, there are annotations for lines of the corresponding colors. Taking "Three-phase Meter27.IA" as an example, it means the current of phase a on line 27. Grid Fault1.Three-phase Meter1.IA represents the short-circuit current of phase a at the fault location.

The microgrid is then switched to islanded mode, and the same fault is applied to bus 11. During the simulations, the islanded microgrid is in the droop-controlled operating mode. The results in the HIL setup are given in Figs. 8 and 9 and the results with the proposed SCC method are presented in Table III. The explanation for Figs. 6 and 7 also applies to Figs. 8 and 9.

Signals Data

find signal

Signal Name	Cursor 1	Cursor 2	Delta	Min.	Max.	Abs.Max.	Mean	RMS
Viewport 1								
Time	0.019708s	0.09249s	0.072782					
Three-phase Meter1.IA	42.828453	64.63475		-63.628483	64.6804	64.6804	-2.8898046	41.588245
Three-phase Meter2.IA	-42.828453	-64.63475		-64.6804	63.628483	64.6804	2.8898046	41.588245
Three-phase Meter3.IA	38.87985	55.064384		-55.2525	55.788143	55.788143	0.11301151	35.72715
Three-phase Meter4.IA	4.128275	9.843391		-21.311182	12.281588	21.311182	-3.0021188	10.468919
Three-phase Meter5.IA	-0.18455045	-0.28525034		-0.8008446	0.79112583	0.8008446	-0.0006086308	0.52571386
Three-phase Meter6.IA	-83.0197	-120.18256		-120.49416	118.76754	120.49416	2.980272	77.507355
Three-phase Meter7.IA	1.1549305	0.40433607		-2.9632523	3.0407908	3.0407908	-0.20585063	1.5533137
Viewport 2								
Time	0.019708s	0.09249s	0.072782					
Three-phase Meter8.IA	39.031456	55.131157		-55.326866	55.86636	55.86636	0.11547112	35.86363
Three-phase Meter9.IA	96.454346	229.87845		-497.18137	286.26077	497.18137	-70.04893	244.13774
Three-phase Meter10.IA	-4.1782484	-6.4565125		-18.115654	17.896023	18.115654	-0.013697689	11.892268
Three-phase Meter11.IA	-1936.9985	-2804.0605		-2811.2905	2771.006	2811.2905	69.54019	1808.342
Three-phase Meter12.IA	27.076155	9.633601		-69.63698	71.45344	71.45344	-4.8026657	36.295
Three-phase Meter13.IA	71.97758	196.6159		-474.41583	275.1101	474.41583	-69.92519	233.84409
Three-phase Meter14.IA	42.337814	59.17646		-109.79697	106.60841	109.79697	-0.36148703	69.82856
Viewport 3								
Time	0.019708s	0.09249s	0.072782					
Three-phase Meter15.IA	-8.930549	-12.956791		-31.30301	30.815443	31.30301	0.11887748	20.5959
Three-phase Meter16.IA	-8.930549	-12.956791		-31.30301	30.815443	31.30301	0.11887748	20.5959
Three-phase Meter17.IA	0.0	0.0		0.0	0.0	0.0	0.0	0.0
Three-phase Meter18.IA	0.0	0.0		0.0	0.0	0.0	0.0	0.0
Three-phase Meter19.IA	-5.617124	-10.88595		-26.273684	25.995594	26.273684	0.016771832	17.29867
Three-phase Meter20.IA	-5.617124	-10.88595		-26.273684	25.995594	26.273684	0.016771832	17.29867
Three-phase Meter21.IA	38.309868	31.405516		-115.237335	117.66	117.66	-4.836207	53.888542
Grid Fault1.Three-phase Meter1.IA	1303.7117	1641.6708		-2790.5505	2723.0093	2790.5505	-50.25226	1863.3422
Viewport 4								
Time	0.019708s	0.09249s	0.072782					
Three-phase Meter22.IA	-20.70793	-30.0438		-72.58425	71.45371	72.58425	0.27563906	47.757023
Three-phase Meter23.IA	-20.70793	-30.0438		-72.58425	71.45371	72.58425	0.27563906	47.757023
Three-phase Meter24.IA	0.0	0.0		0.0	0.0	0.0	0.0	0.0
Three-phase Meter25.IA	0.0	0.0		0.0	0.0	0.0	0.0	0.0
Three-phase Meter26.IA	-13.02467	-25.241922		-60.922077	60.277252	60.922077	0.03889097	40.111263
Three-phase Meter27.IA	-13.02467	-25.241922		-60.922077	60.277252	60.922077	0.03889097	40.111263

Fig. 8. RMS values of currents on lines 1-27 under 3LG fault in HIL setup when microgrid is in islanded mode.

The CPU time needed for SCC execution is 0.225 s in real-life example that implies the microgrid connected to the 186-bus feeder. The location of fault does not affect the CPU time needed.

Furthermore, the proposed SCC method is applied to the 9-bus microgrid from [23], as shown in Fig. 10, for comparison with one of the state-of-the-art methods. The 9-bus microgrid is an islanded microgrid [23]. The comparison of results obtained by method in [23] and proposed SCC method are given in Table IV, where only the results for SLG and 3LG faults are presented due to space limitations.

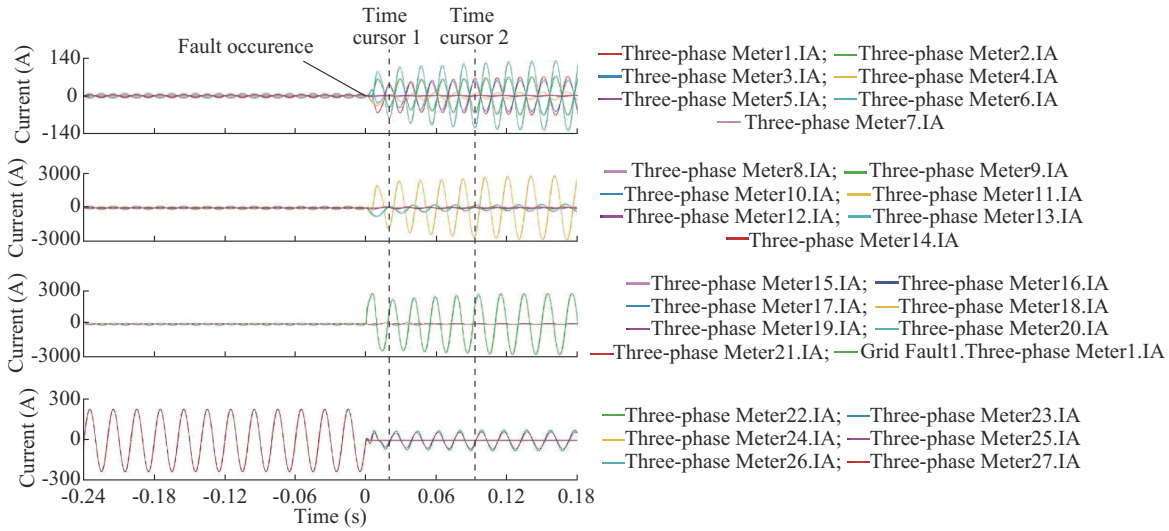

Fig. 9. Time-domain currents on lines 1-27 under 3LG fault in HIL setup when microgrid is in islanded mode.

TABLE III
CURRENTS ON LINES 1-27 UNDER 3LG FAULT WITH PROPOSED SCC METHOD WHEN MICROGRID IS IN ISLANDED MODE

Fault current	Phase a		Phase b		Phase c	
	Magnitude (A)	Angle (°)	Magnitude (A)	Angle (°)	Magnitude (A)	Angle (°)
I_1	42.12	115.21	42.12	−4.79	42.12	−124.79
I_2	42.12	−76.46	42.12	163.54	42.12	43.54
I_3	35.42	111.30	35.42	−8.70	35.42	−128.70
I_4	10.88	−88.86	10.88	151.14	10.88	31.14
I_5	0.72	−24.95	0.72	−144.95	0.72	95.05
I_6	78.01	−71.50	78.01	168.50	78.01	48.50
I_7	1.65	−85.05	1.65	154.95	1.65	34.95
I_8	35.22	111.29	35.22	−8.71	35.22	−128.70
I_9	248.64	−88.86	248.64	151.14	248.64	31.14
I_{10}	11.10	−24.96	11.10	−144.96	11.10	95.04
I_{11}	1815.09	−71.50	1815.09	168.50	1815.09	48.50
I_{12}	35.52	−85.05	35.52	154.95	35.52	34.95
I_{13}	229.23	−93.19	229.23	146.81	229.23	26.81
I_{14}	68.51	−93.98	68.51	146.02	68.51	26.02
I_{15}	21.12	−50.32	21.12	−170.32	21.12	69.69
I_{16}	21.12	−50.32	21.12	−170.32	21.12	69.69
I_{17}	0	0	0	0	0	0
I_{18}	0	0	0	0	0	0
I_{19}	17.88	−52.36	17.88	−172.36	17.88	67.64
I_{20}	17.88	−52.36	17.88	−172.36	17.88	67.64
I_{21}	52.95	−96.24	52.95	143.76	52.95	23.76
I_{22}	46.95	−50.32	46.95	−170.32	46.95	69.68
I_{23}	46.95	−50.32	46.95	−170.32	46.95	69.68
I_{24}	0	0	0	0	0	0
I_{25}	0	0	0	0	0	0
I_{26}	40.72	−52.36	40.72	−172.36	40.72	67.64
I_{27}	40.72	−52.36	40.72	−172.36	40.72	67.64

Ultimately, the results obtained by the proposed SCC method under the following two conditions of complex short-circuit faults in the microgrid on CWRU campus are presented in Table V and Table VI, respectively. Due to space limitations, only the currents for four representative lines are presented.

Condition 1: simultaneous LL-G fault (phases bc) at bus 5 and L-G fault (phase a) at bus 10. The microgrid is in the

grid-connected mode.

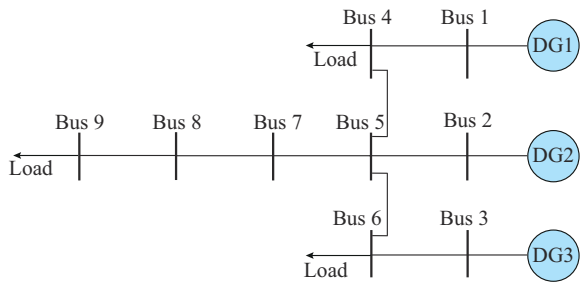

Fig. 10. Structure of 9-bus microgrid.

Condition 2: simultaneous L-G fault (phase a) with fault impedance 0.01 Ω at bus 10 and L-G fault (phase b) at bus 10. The microgrid is in the grid-connected mode.

From the aforementioned results, the following conclusion can be obtained.

1) It can be observed from Table II and Figs. 6 and 7 that the proposed SCC method can efficiently solve the fault current of grid-connected microgrids and it provides highly accurate results. The slight differences (less than 1%) between the proposed SCC method and the HIL setup are attributed to different modeling of loads. The HIL calculates fault currents in the time domain and then derives the RMS values, whereas the proposed SCC method is completely executed in the complex domain as it is intended for industrial use and needs to be time-saving. The principal motive for benchmarking the proposed SCC method against HIL setup is to validate its accuracy. HIL is renowned for its high-fidelity and precise responses, making it an ideal testbed. As demonstrated, the proposed SCC method could yield exceptionally accurate results, closely aligning with those obtained via HIL setup. Additionally, it could complete the calculation within milliseconds, much more efficient than HIL setup, which take minutes for smaller microgrids and potentially hours for larger ones to deliver results. Thus, the proposed SCC method effectively meets both critical criteria for industrial computational methods: accuracy and rapid response. This alignment with the key requirements underscores the significance and applicability of the proposed SCC method in industrial settings.

2) It can be observed from Table III and Figs. 8 and 9 that the proposed SCC method solves the fault currents of islanded microgrids with the same efficiency and robustness, and it overcomes the limitations of BFS methods for islanded microgrids without a stiff slack-bus (network root). Again, there are also slight differences between the proposed method and the HIL setup (less than 1%).

TABLE IV
COMPARISON RESULTS OBTAINED BY METHOD IN [23] AND PROPOSED SCC METHOD

Location	Method	Fault current under SLG (A)			Fault current under 3LG (A)			The maximum difference (%)
		Phase a	Phase b	Phase c	Phase a	Phase b	Phase c	
Bus 8	[23]	527.0	0	0	539.0	539.0	539.0	1.15
	Proposed	531.2	0	0	545.2	545.2	545.2	
DG1	[23]	182.7	21.5	22.3	186.1	186.1	186.1	0.93
	Proposed	179.5	21.3	22.1	185.3	185.3	185.3	
DG2	[23]	187.5	24.6	22.8	195.2	195.2	195.2	2.03
	Proposed	186.6	24.1	22.4	193.5	193.5	193.5	
DG3	[23]	182.7	21.5	22.3	186.1	186.1	186.1	0.93
	Proposed	179.5	21.3	22.1	185.3	185.3	185.3	

TABLE V
SCC RESULTS FOR COMPLEX SHORT-CIRCUIT FAULTS UNDER CONDITION 1

Fault current	Phase a		Phase b		Phase c	
	Magnitude (A)	Angle (°)	Magnitude (A)	Angle (°)	Magnitude (A)	Angle (°)
I_1	359.94	–70.70	442.24	157.93	442.17	37.92
I_2	1.84	–170.95	1.67	62.85	1.77	–59.05
I_5	364.27	–68.87	444.34	159.48	444.34	39.49
I_{10}	8499.56	–68.87	0	0	0	0

TABLE VI
SCC RESULTS FOR SHORT-CIRCUIT FAULTS UNDER CONDITION 2

Fault current	Phase a		Phase b		Phase c	
	Magnitude (A)	Angle (°)	Magnitude (A)	Angle (°)	Magnitude (A)	Angle (°)
I_1	310.31	–56.22	359.40	169.32	9.95	–59.68
I_2	1.71	–176.19	1.90	62.27	1.59	–34.81
I_5	317.73	–54.44	364.26	171.13	2.06	119.71
I_{10}	7413.61	–54.44	8499.44	171.13	48.02	119.71

3) It is obvious from Table IV that the results from the state-of-the-art method [23] and the proposed SCC method are almost identical (the difference is less than 2.03%). It means that the proposed SCC method is equally efficient for microgrid in islanded mode as the method from [23]. Moreover, the proposed SCC method offers a notable benefit in that it is equally accurate for grid-connected and utility microgrids, which are not within the scope of [23]. Another significant aspect of the proposed SCC method is the progress made in managing negative and zero sequences in IBDER fault currents. In other methods that use generalized Δ-circuit, such as [1] and [9], only instantaneous saturation limit strategy and latched limit strategy are taken into account, which means that only positive-sequence injections of IBDER are considered. Till now, there is no evidence that the methods based on the generalized Δ-circuit concept are capable of taking into account all DER models, regardless of their control strategies including virtual impedance current limiters. In Table IV, the fault contributions of IBDERs are not balanced under the SLG (unbalanced fault). This is dictated by the control strategy and the proposed SCC method is capable of accounting for that.

4) The results from Tables V and VI show that the proposed SCC method is fully capable of solving arbitraryly-selected complex short-circuit faults with the same simplicity, which is an essential feature for industrial software tools, such as advanced distribution management systems (ADMSs), distributed energy resource management systems (DERMSs), and microgrid management systems (MMSs). These tools need to provide DSOs, grid engineers, and microgrid controllers with robust computations that are able to cope with all types of complex faults that may occur in the field. Thus, it is of utmost importance to have a robust SCC method that can solve any type of complex short-circuit faults, accurately set and coordinate the protection equipment in the microgrid, and properly locate the faulted bus to react in a timely manner to clear the fault. For this purpose, the proposed SCC method can be particularly useful without requiring predefinition of boundary conditions for each of different fault types. This ability differentiates the proposed SCC method from other SCC methods.

Finally, as presented on a real-life example of a 186-bus feeder with a connected microgrid, besides islanded and grid-connected microgrids owned and operated by third-party aggregators, the proposed SCC method is able to efficiently calculate faulted microgrids as parts of utility grids and thus, it offers DSOs a reliable and efficient tool for implementation in advanced applications such as adaptive relay protection and FLISR.

VIII. Conclusion

In this paper, a robust and highly accurate SCC method for microgrids is proposed, regardless of their operational state, topology, and ownership, affected by any kind of complex short-circuit faults.

The proposed SCC method is efficient for microgrids in both islanded and grid-connected modes as well as utility microgrids as part of a larger distribution grid, with the same simplicity. As the proposed SCC method is based on the admittance matrix of the faulted system, it does not need a stiff slack bus (network root), and thus overcomes the limitations of BFS methods.

Further, the proposed SCC method solves all types of complex short-circuit faults with the same simplicity, without the need to predefine fault conditions for each of different fault types. This differentiates the proposed method from other SCC methods for microgrids.

Finally, the robustness and efficiency of the proposed SCC method make it particularly useful for advanced applications in industrial software tools for grid management, such as ADMS, DERMS, and MMS [28]-[30].

References

[1] L. Strezoski, M. Prica, and K. A. Loparo, "Sequence domain calculation of active unbalanced distribution systems affected by complex short circuits," *IEEE Transactions on Power Systems*, vol. 33, no. 2, pp. 1891-1902, Mar. 2018.
[2] P. M. Anderson, *Analysis of Faulted Power Systems*. New York: IEEE Press, 1995.
[3] R. Bergen and V. Vittal, *Power System Analysis.* New Jersey: Prentice Hall, 2000.
[4] V. C. Strezoski and D. D. Bekut, "A canonical model for the study of faults in power systems," *IEEE Transactions on Power Systems*, vol. 6, no. 4, pp. 1493-1499, Nov. 1991.
[5] X. Zhang, F. Soudi, D. Shirmohammadi *et al*., "A distribution short circuit analysis approach using hybrid compensation method," *IEEE Transactions on Power Systems*, vol. 10, no. 4, pp. 2053-2059, Nov. 1995.
[6] W. Lin and T. Ou, "Unbalanced distribution network fault analysis with hybrid compensation," *IET Generation*, *Transmission & Distribution*, vol. 5, no. 1, p. 92, Dec. 2011.
[7] J. Teng, "Systematic short-circuit-analysis method for unbalanced distribution systems," *IEE Proceedings*: *Generation*, *Transmission and Distribution*, vol. 152, no. 4, p. 549, Jul. 2005.
[8] J. Teng, "Unsymmetrical short-circuit fault analysis for weakly meshed distribution systems," *IEEE Transactions on Power Systems*, vol. 25, no. 1, pp. 96-105, Feb. 2010.
[9] L. Strezoski, M. Prica, and K. A. Loparo, "Generalized Δ-circuit concept for integration of distributed generators in online short-circuit calculations," *IEEE Transactions on Power Systems*, vol. 32, no. 4, pp. 3237-3245, Jul. 2017.
[10] R. A. Jabr and I. Džafić, "A fortescue approach for real-time short circuit computation in multiphase distribution networks," *IEEE Transactions on Power Systems*, vol. 30, no. 6, pp. 3276-3285, Nov. 2015.
[11] M. Ghanaatian and S. Lotfifard, "Sparsity-based short-circuit analysis of power distribution systems with inverter interfaced distributed generators," *IEEE Transactions on Power Systems*, vol. 34, no. 6, pp. 4857-4868, Nov. 2019.
[12] I. Kim, "Short-circuit analysis models for unbalanced inverter-based distributed generation sources and loads," *IEEE Transactions on Power Systems*, vol. 34, no. 5, pp. 3515-3526, Sept. 2019.
[13] N. Simic, L. Strezoski, and B. Dumnic, "Short-circuit analysis of DER-based microgrids in connected and islanded modes of operation," *Energies*, vol. 14, no. 19, p. 6372, Oct. 2021.
[14] T. C. Mosetlhe, O. M. Babatunde, T. R. Ayodele *et al*., "Fault analysis in a grid-tied microgrid system," in *Proceedings of 2022 30th Southern African Universities Power Engineering Conference*, Durban, South Africa, Jan. 2022, pp. 1-4.
[15] S. Ghosh, C. K. Chanda, and J. K. Das, "Performance analysis of a grid connected microgrid system under fault condition," *Microsystem Technologies*, vol. 28, no. 12, pp. 2689-2696, Apr. 2022.
[16] T. Ghanbari and E. Farjah, "Unidirectional fault current limiter: an efficient interface between the microgrid and main network," *IEEE Transactions on Power Systems*, vol. 28, no. 2, pp. 1591-1598, May 2013.
[17] U.S. Department of Energy Office of Scientific and Technical Information. (2017, May). Fault analysis and detection in microgrids with high PV penetration. [Online]. Available: https://doi.org/10.2172/1367437
[18] Z. Wang, L. Mu, Y. Xu *et al*., (2021, Apr.). The fault analysis method

of islanded microgrid based on the *U/f* and *PQ* control strategy. [Online]. Available: https://doi.org/10.1002/2050-7038.12919

[19] L. Strezoski, "Distributed energy resource management systems – DERMS: state of the art and how to move forward," *WIREs Energy and Environment*, vol. 12, no. 1, pp. 1-21, Jan. 2023.

[20] L. V. Strezoski, B. Dumnic, B. Popadic *et al*., "Novel fault models for electronically coupled distributed energy resources and their laboratory validation," *IEEE Transactions on Power Systems*, vol. 35, no. 2, pp. 1209-1217, Mar. 2020.

[21] M. Patel, "Opportunities for standardizing response, modeling and analysis of inverter-based resources for short circuit studies," *IEEE Transactions on Power Delivery*, vol. 36, no. 4, pp. 2408-2415, Aug. 2021.

[22] A. Haddadi, E. Farantatos, M. Patel *et al*., "Need for load modeling in short circuit analysis of an inverter-based resource-dominated power system," *IEEE Transactions on Power Delivery*, vol. 38, no. 3, pp. 1882-1890, Jun. 2023.

[23] E. E. Pompodakis, L. Strezoski, N. Simic *et al*., "Short-circuit calculation of droop-controlled islanded AC microgrids with virtual impedance current limiters," *Electric Power Systems Research*, vol. 218, p. 109184, May 2023.

[24] L. Strezoski, I. Stefani, and D. Bekut, "Novel method for adaptive relay protection in distribution systems with electronically-coupled DERs," *International Journal of Electrical Power & Energy Systems*, vol. 116, p. 105551, Mar. 2020.

[25] S. Parhizi, H. Lotfi, A. Khodaei *et al*., "State of the art in research on microgrids: a review," *IEEE Access*, vol. 3, pp. 890-925, Jun. 2015.

[26] M. Hong. (2014, Jul.). The Case Western Reserve University campus microgrid. [Online]. Available: https://www.energy.gov/sites/prod/files/2014/07/f18/CaseWesternReserveUniversityCampusGrid.pdf

[27] N. Simić, L. Strezoski, and R. Milićević, "Relay protection in microgrids: settings and sensitivity in presence of IBDERs," in *Proceedings of 2022 IEEE PES Innovative Smart Grid Technologies Conference Europe*, Novi Sad, Serbia, Oct. 2022, pp. 1-5.

[28] L. Strezoski, H. Padullaparti, F. Ding *et al*., "Integration of utility distributed energy resource management system and aggregators for evolving distribution system operators," *Journal of Modern Power Systems and Clean Energy*, vol. 10, no. 2, pp. 277-285, Mar. 2022.

[29] L. Strezoski, I. Stefani, and B. Brbaklic, "Active management of distribution systems with high penetration of distributed energy resources," in *Proceedings of IEEE EUROCON 2019 – 18th International Conference on Smart Technologies*, Novi Sad, Serbia, Jul. 2019, pp. 1-5.

[30] L. V. Strezoski, N. R. Vojnovic, V. C. Strezoski *et al*., "Modeling challenges and potential solutions for integration of emerging DERs in DMS applications: power flow and short-circuit analysis," *Journal of Modern Power Systems and Clean Energy*, vol. 7, no. 6, pp. 1365-1384, Nov. 2019.

Luka V. Strezoski received the B.S., M.Sc., and Ph.D. degrees (with honors) in power engineering from the University of Novi Sad, Novi Sad, Serbia, in 2013, 2014, and 2017, respectively. His Ph.D. research was conducted under joint supervision between the University of Novi Sad and Case Western Reserve University, Cleveland, USA. He is currently with the Faculty of Technical Sciences, University of Novi Sad, as an Associate Professor and the Head of the Power Engineering and Applied Software Department and the Director of the Smart Grid Laboratory. He is also a Visiting Affiliate with Case Western Reserve University. His current research interests include distribution system modeling, renewable distribution generation modeling, and integration of distributed energy resources (DERs) into the distribution management system (DMS) and distributed energy resource management system (DERMS) applications.

Nikola G. Simic received the B.S. and M.S. degrees in power engineering from the University of Novi Sad, Novi Sad, Serbia, in 2016 and 2018, respectively. Now, he is the Ph.D. Candidate and Teaching Assistant at the same university. His current research interests include integration of DERs into modern power systems and microgrids, as well as development and implementation of advanced distribution management system (ADMS) and DERMS applications.

Kenneth A. Loparo is the Arthur L. Parker Professor Emeritus and the Founder and Faculty Director of Institute for Smart, Secure and Connected Systems (ISSACS) at Case Western Reserve University, Cleveland, USA. He is an IEEE Life Fellow, Distinguished IIAV Fellow, and AIMBE Fellow. His current research interests include stability and control of nonlinear systems with applications to large-scale electric power systems, nonlinear filtering with applications to monitoring, fault detection, diagnosis, and reconfigurable control.